PHYSICAL REVIEW B VOLUME 49, NUMBER 19 15 MAY 1994-I

Determination of the electron density in $GaAs/Al_xGa_{1-x}As$ heterostructures

J. Martorell
Departamento d'Estructura i Constituents de la Materia, Facultat de Física, University of Barcelona, Barcelona 08028, Spain

D. W. L. Sprung
Department of Physics and Astronomy, McMaster University, Hamilton, Ontario, Canada L8S 4M1
(Received 10 November 1993)

An optimized self-consistent method for determination of the quantal electron density is presented. It is applied, in the zero-temperature case, to devices with either partial or full donor ionization. A Thomas-Fermi approximation for the $T = 0$ limit is developed and shown to be appropriate for systematic studies of the two-dimensional electron density, σ_-. A suitable linear approximation is found that provides simple and accurate analytic expressions for σ_- in terms of the physical parameters of the device.

I. INTRODUCTION

In appropriately doped planar $GaAs/Al_xGa_{1-x}As$ heterostructures a quasi-two-dimensional electron gas (2DEG) forms at the interface between spacer and substrate. Its properties have been thoroughly studied both theoretically and experimentally in recent years. The foundations of the work on this subject were laid by Stern and collaborators in their earlier study of the $GaAs/Al_xGa_{1-x}As$ junction, [see (Ref. 1) and references therein] where the reliability of several of the approximations currently used for heterostructures is carefully discussed. A recent and representative quantal calculation of the electron gas distribution in a heterojunction is presented in Sec. IV B of Ref. 2. The interest in heterostructures has increased recently since they form the basis of more complex devices like single or multiple quantum wires and quantum dots. A better understanding of these more complex systems requires having not only a good quantitative description of the properties of the electron gas in the simple, ungated, planar heterostructures but also an easy interpretation of the role of the different physical quantities in determining these properties. These are the objectives of this work.

We will first focus on improving the efficiency of the currently used iterative approach, and second we will show that the Thomas-Fermi approximation provides analytic expressions that clarify the physics relevant to the problem, while still being sufficiently accurate for a quantitative comparison with data on the two-dimensional electron density.

For simplicity we shall treat only the zero-temperature case, although most of the results of Sec. II are easily extended to finite temperatures, as will be briefly discussed. It is, however, important to remark that our model applies only when the device is in thermodynamic equilibrium, i.e., when the Fermi level is the same at all points. This requirement may be difficult to guarantee in experimental devices at low temperatures due to the special properties of the DX centers, which lead to rather long times for capture or emission of the electrons by the donors. A meaningful comparison with experiment can be made only when these specific equilibrium conditions are guaranteed. To enlarge the domain of application of our methods we have included, as one of our particular cases, a model with two kinds of donors, deep and shallow, which has been proposed as a valid approximation to realistic conditions in some experimental devices.[3]

In principle, the determination of the density of electrons in the spacer and substrate layers requires use of an iterative method. One solves the Poisson equation in the whole heterostructure, to determine the electrostatic potential acting on the electrons in the conduction band, and then the Schrödinger equation for that potential. This is repeated until convergence to stable values. In the usual heterostructure geometry the donors and the 2DEG are well separated by a spacer layer, so that in the cap and donor layers the Poisson equation can be integrated analytically, and in the other layers the solution can be written explicitly in terms of a quadrature on the electron density. In this work we will exploit this fact to simplify that step of the iterative process. We will show how this simplification can be applied not only to improve the iterative solution in the case when all the donors are ionized, as in the model of Ref. 2, but also when some parts of the donor layer are not fully ionized, a situation which often happens in experimental devices.[4]

Next, by introducing the Thomas-Fermi (TF) approximation for the electrons in the 2DEG we will show that the 2D density can be computed with good accuracy and much less numerical effort than in the iterative process. The TF approximation allows one to treat equally easily the partially and the fully ionized donor layer cases, replacing all the numerics of the self-consistent process by a determination via the Newton-Raphson method of the zeroes of an analytic function. Finally, by introducing an appropriate linear approximation we will derive accurate analytic expressions for the 2D density, which allow a very simple visualization of the role of the different physical quantities in its determination. This makes

0163-1829/94/49(19)/13750(10)/$06.00 ©1994 The American Physical Society

the study of systematic trends very simple.

In the last two sections of this work we will extend the method to the cases when (i) a gate at negative potential covers the surface completely, and (ii) there is a small concentration of acceptor states in the substrate. We will show that the same approximations are applicable to these devices.

II. THE SELF-CONSISTENT APPROACH

Case 1: Fully ionized donors. We begin with the simplest case: that of a conventional planar heterostructure like the one considered in Ref. 2, where the full donor and cap layers are ionized. The details of that heterostructure are given in their Fig. 3: Starting from the exposed surface, there are (i) a GaAs cap layer, of thickness c and doped with a constant donor number density ρ_c, (ii) an $Al_xGa_{1-x}As$ donor layer, of thickness d and doped with a constant number density ρ_d, (iii) an $Al_xGa_{1-x}As$ undoped spacer layer of thickness s, and (iv) a thick GaAs substrate layer. We choose the z axis perpendicular to the layers, with the origin at the exposed surface. As is customary we assume that the surface states produce Fermi level pinning, and choose the energy of the electrons trapped in these states as the reference zero of energies, thus setting to zero the Fermi level energy of the 2DEG. We shall write as $e\phi_s$ the binding energy of these states with respect to the bottom of the conduction band. For the device parameters considered in Ref. 2 the conduction band energy, as shown in their Fig. 4, is such that all the donors are ionized, and the electrons distribute themselves between the 2DEG, with number density $\rho_e(z)$, and the surface states, with surface number density σ_s. The electrostatic potential resulting from the integration of the Poisson equation is analytic in the cap and donor layers, so that including the boundary conditions at the surface, the energy of an electron at the bottom of the conduction band is

$$e\Phi(0 < z \leq z_1) = e\phi_s - e^2\frac{\sigma_s}{\varepsilon_1}z + e^2\frac{\rho_c}{2\varepsilon_1}z^2, \quad (1)$$

$$\begin{aligned} e\Phi(z_1 < z \leq z_2) = {} & e\Phi(z_1) - e^2\frac{\sigma_s}{\varepsilon_2}(z - z_1) \\ & + e^2\frac{\rho_c}{\varepsilon_2}z_1(z - z_1) \\ & + e^2\frac{\rho_d}{2\varepsilon_2}(z - z_1)^2 + e\Phi_b, \end{aligned} \quad (2)$$

where we have defined $z_1 = c$, $z_2 = c + d$ and $e\Phi_b$ is the discontinuity due to the band offset between the two materials. The dielectric constants are written as ε_1 for GaAs and ε_2 for $Al_xGa_{1-x}As$. At the boundaries between the two materials the continuity of the potential and of the normal component of the electric displacement has been imposed. Since the electron density is nonvanishing in the spacer and the substrate, the corresponding expressions require a quadrature:

$$\begin{aligned} e\Phi(z_2 < z \leq z_3) = {} & e\Phi(z_2) + e\Phi'(z_2)(z - z_2) \\ & - \frac{e^2}{\varepsilon_2}\int_{z_2}^{z} dz'\,(z - z')\rho_e(z') \\ & + e\Phi_{\mathrm{exch}}(z), \end{aligned} \quad (3)$$

$$\begin{aligned} e\Phi(z_3 < z) = {} & e\Phi(z_3) - e\Phi_b + \frac{\varepsilon_2}{\varepsilon_1}e\Phi'(z_3 - 0)(z - z_3) \\ & - \frac{e^2}{\varepsilon_1}\int_{z_3}^{z} dz'\,(z - z')\rho_e(z') + e\Phi_{\mathrm{exch}}(z), \end{aligned} \quad (4)$$

where $z_3 \equiv z_2 + s$, and exchange effects are included either in the Slater approximation

$$e\Phi_{\mathrm{exch}}(z) = -\frac{e^2}{4\pi\varepsilon(z)}\left(\frac{3\rho_e(z)}{\pi}\right)^{1/3}, \quad (5)$$

or in the Hedin and Lundqvist[5] parametrization as proposed by Stern and Das Sarma.[1] The latter takes account of correlation effects as well. It can be easily checked that the charge neutrality condition is

$$\sigma_s + \sigma_- = \rho_c c + \rho_d d, \quad (6)$$

where

$$\sigma_- = \int_{z_2}^{\infty} \rho_e(z)dz. \quad (7)$$

This guarantees that the electric field vanishes when $z \to \infty$, as it should. Equations (1) to (7) determine the potential completely once $\rho_e(z)$ is known. The latter is computed from the solutions, $\Psi_n(z)$, of the Schrödinger equation:

$$-\frac{\hbar^2}{2}\frac{d}{dz}\frac{1}{m^*(z)}\frac{d\Psi_n}{dz} + e\Phi(z)\Psi_n(z) = E_n\Psi_n(z) \quad (8)$$

and the occupation factors ν_n per unit area correspond to free motion in the x-y plane. For a finite temperature, T, they are given by

$$\nu_n = \frac{m^*(z)k_BT}{\pi\hbar^2}\ln\left[1 + \exp\left(\frac{E_F - E_n}{k_BT}\right)\right], \quad (9)$$

where in our convention $E_F = 0$. We shall restrict our study to devices operated at temperatures of a few kelvin. Then the zero-temperature occupations can be safely used in the determination of the electron density and we write

$$\rho_e(z) = \sum_{n\in \mathrm{b.s.}} |E_n|\frac{m^*(z)}{\pi\hbar^2}|\Psi_n(z)|^2, \quad (10)$$

with the sum extended over the bound states and the wave functions $\Psi_n(z)$ are normalized to unity. For the rounding off of the discontinuities due to the band offsets we follow the method of Stern and Das Sarma.[1]

Since the potential is an input to the Schrödinger equation, the determination of ρ_e and $e\Phi$ must be done iteratively. One makes an initial choice for $e\Phi(z)$ (we choose the Thomas-Fermi solution as described in the next section), obtains $\rho_e(z)$ from Eqs. (8)–(10), and σ_- and σ_s from Eqs. (6) and (7), and finally substitutes these into

Eqs. (1)–(5) to generate a new $e\Phi$. Then the process is repeated until convergence to stable values. The self-consistent solutions that we obtain in this way for the device of Ref. 2 are shown in Fig. 1(a) for our choice of parameters: $e\phi_s = 0.67$ eV, $e\Phi_b = 0.23$ eV, $\varepsilon_{r,1} = 13.2$, $\varepsilon_{r,2} = 12.2$, $m_1^*/m = 0.067$, and $m_2^*/m = 0.088$. The agreement with Fig. 4 of Ref. 2 is quite satisfactory. In our calculation the effect of the exchange terms was included in the Hedin and Lundqvist (HL) approximation. However, the differences in the shape are negligible if the simpler Slater approximation is used instead. In Table I we give our result for the two-dimensional electron density σ_- using the HL parametrization. This will be used as reference for the further approximations to be introduced in later sections. The effect of using one or the other prescription for the exchange terms is very small: with the Slater approximation we find $\sigma_- = 0.0026$ nm^{-2}, the same value found when exchange effects are completely neglected.

Case 2: Only one kind of donor, partially ionized. Depending on the geometrical parameters of the device and the amount of doping, the minimum energy of the conduction band in the donor layer could be so low that for some z it would be lower than the energy required to ionize the donors; then the assumption of complete ionization of the donor layer is no longer appropriate. As an example of this kind of device we study the heterostructure used by Laux *et al.*[6] as a starting point for their quantum wire calculations. In their model the donors have a unique ionization energy $e\Phi_i = 0.05$ eV and the sizes of the different layers and the amount of doping can be found in that reference. We will omit in this section the effect of the acceptor states in the substrate, which will be treated later, in Sec. V. Under these conditions there is a zone inside the donor layer, $z_l < z < z_r$, where the donors retain their electrons, and there is no net charge in it. The bottom of the conduction band is flat, $e\Phi(z) = e\Phi_i$, and there is no electric field. For that the left ionized part of the donor layer, $[z_1, z_l]$, plus the cap layer, must have the same number of charges as the surface:

$$\sigma_s = \rho_c z_1 + \rho_d (z_l - z_1); \tag{11}$$

and the right ionized part of the donor layer, $[z_r, z_2]$, must have the same charge as the 2DEG:

$$\sigma_- = \rho_d (z_2 - z_r). \tag{12}$$

TABLE I. Two-dimensional electron densities for several devices: case 1, Tan *et al.*; case 2, Laux *et al.*; case 3, Fletcher *et al.* The different approximations are discussed in the text.

σ_-	Case 1	Case 2	Case 3 Set 1	Case 3 Set 2
Fully quantal	0.0027	0.0046	0.0060	0.0062
Thomas-Fermi	0.0026	0.0051	0.0069	0.0069
TF + linear	0.0027	0.0052	0.0063	0.0065

In this situation there are two completely decoupled sets of conditions that determine the equilibrium charges for the surface and the 2DEG: for the external part of the device, $0 < z \leq z_l$, Eqs. (1) and (2) apply, and the values of z_l and σ_s are determined by Eq. (11) and the condition

$$e\Phi(z_l) = e\Phi_i. \tag{13}$$

The solution is analytic:

$$z_l = \left(1 - \frac{\varepsilon_2}{\varepsilon_1}\right) z_1 + \sqrt{z_1^2 \frac{\varepsilon_2^2}{\varepsilon_1^2}\left(1 - \frac{\varepsilon_1 \rho_c}{\varepsilon_2 \rho_d}\right) + \frac{2\varepsilon_2\, e(\phi_s + \Phi_b - \Phi_i)}{e^2 \rho_d}}, \tag{14}$$

with σ_s given by Eq. (11). For the zone, $[z_r, \infty]$, the solution is obtained via a self-consistent process analogous to that in the full ionization case, but now the condition for charge conservation is Eq. (12) instead of (6) and the potential in the zone $[z_r, z_2]$ is written as

$$e\Phi(z) = e\Phi_i + e^2 \frac{\rho_d}{2\varepsilon_2}(z - z_r)^2. \tag{15}$$

The iterative solution is started with an initial guess for the electrostatic field, $e\Phi(z)$, in the spacer and substrate (which we again choose as the solution in the Thomas-Fermi approximation.) Next the Schrödinger equation is solved and the electron densities are constructed using Eqs. (10) and (7). From Eq. (12) a value for z_r is determined and the electrostatic field is computed from Eqs. (15) and (4). Then the whole process is repeated until stable values are obtained.

Results given by this self-consistent method are shown in Fig. 1(b). Our computed value for the two-dimensional charge density, σ_- of Eq. (7), for the model

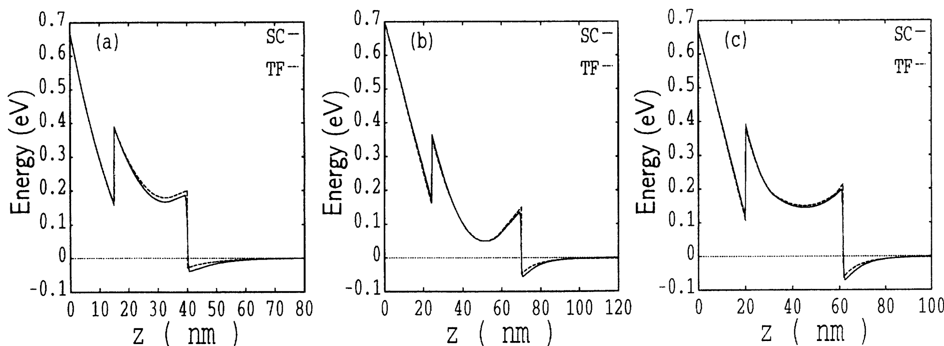

FIG. 1. (a) Conduction band edge for the device of Tan *et al.* (Ref. 2), the continuous line is the fully quantal result, whereas the dashed line is the prediction of the Thomas-Fermi approximation. (b) Same for the device of Laux *et al.* (Ref. 6) and (c) same for the device of Fletcher *et al.* (Ref. 3).

device studied by Laux *et al.*[6] is given in Table I. We use the same parameter set as in that reference, but again include the Coulomb exchange effect in the Hedin-Lundqvist parametrization. When we omit that term our value is changed to $\sigma_- = 0.0044\ \text{nm}^{-2}$, in agreement with that found by Laux *et al.* We shall see in Sec. V that the inclusion of a small density of acceptor states does not change this value.

The above analytic expressions show explicitly a remarkable property of case 2 devices: any increase in the thickness of the donor layer above the critical value for which the neutral zone appears, leaves unchanged all the properties of the 2DEG, so that they behave as single junctions, decoupled from the surface.

Case 3: Two kinds of donor states, shallow and deep, the latter partially ionized. To get closer to the experimental conditions of some devices we now study a model introduced by Fletcher *et al.* in Ref. 3. These authors allow for two kinds of states in the donor layer: shallow and deep. The binding energy for the shallow state is assumed to be negligible, and that of the deep state will be written as $e\Phi_x$. The densities of both kinds of states will be written as ρ_s and ρ_x and their sum by ρ_d as before. As in the previous case, we will not include the effect of the acceptor states, which is left for Sec. V.

In the zone $0 < z \leq z_l$, Eqs. (1) and (2) still apply, and the position of z_l is now determined by the condition that the energy of the conduction band should equal the binding energy of the deep donors. Here we use this condition to relate σ_s to z_l:

$$\sigma_s = \rho_c z_1 + \frac{e\bar{\Phi} + \frac{e^2}{2\varepsilon_2}\rho_d u^2}{e^2\left(\frac{z_1}{\varepsilon_1} + \frac{u}{\varepsilon_2}\right)}, \tag{16}$$

where we have introduced auxiliary quantities by defining

$$u = z_l - z_1, \tag{17}$$

$$e\bar{\Phi} = e\phi_s - \frac{e^2}{2\varepsilon_1}\rho_c z_1^2 + e\Phi_b - e\Phi_x.$$

Now in the zone $[z_l, z_r]$ only the shallow donor states are ionized, so that

$$e\Phi(z_l \leq z \leq z_r) = e\Phi_x - \frac{e^2}{\varepsilon_2}(\sigma_s - \rho_c z_1 - \rho_d u)(z - z_l) + \frac{e^2}{2\varepsilon_2}\rho_s (z - z_l)^2, \tag{18}$$

and the point z_r is again determined by the condition of the equality of the conduction band energy and $e\Phi_x$. This gives

$$z_r = z_l + \frac{2}{\rho_s}(\sigma_s - \rho_c z_1 - \rho_d u). \tag{19}$$

Note that in this case the positive charge in the central zone, $[z_l, z_r]$, is exactly twice the net negative charges in the left and in the right zones, *which are equal.* Note also that when $\rho_s \to 0$ the results of the previous case are easily recovered. Finally, in the remainder of the donor layer

$$e\Phi(z_r < z \leq z_2) = e\Phi_x + \frac{e^2}{\varepsilon_2}(\sigma_s - \rho_c z_1 - \rho_d u)(z - z_r) + \frac{e^2}{2\varepsilon_2}\rho_d (z - z_r)^2, \tag{20}$$

and in the spacer and substrate, Eq. (3) again applies. The charge neutrality condition reads:

$$\sigma_- + \sigma_s = \rho_c c + \rho_d d - \rho_x (z_r - z_l). \tag{21}$$

We again start the iterative solution with the Thomas-Fermi as an initial guess for the electrostatic field. Then from the solutions of the Schrödinger equation the electron densities $\rho_e(z)$ and σ_- are constructed. Using Eqs. (16) and (19) it is easy to check that the charge neutrality condition Eq. (21) determines implicitly a new u. We determine it using the Newton-Raphson algorithm and then from Eqs. (16) and (19) determine a new set of values of σ_s, z_l, and z_r that allow one to construct the new field. The sequence is then repeated until stable values are obtained.

We take here as a reference the device of Fletcher *et al.*, and more specifically choose two of the sets of values of $e\Phi_x$ and $r \equiv \rho_s/\rho_x$, from their Table II. The first set corresponds to the device shown in their Fig. 8: $e\Phi_x = 0.180$ eV, $r = 0.269$, and the second to $e\Phi_x = 0.190$ eV, $r = 0.430$. Our self-consistent solution for the conduction band profile is shown in Fig. 1(c) for the first parameter set, results for σ_- for both sets are given in Table I. Here the differences due to the Coulomb exchange contribution are more sizeable: omitting that term we find $\sigma_- = 0.0056\ \text{nm}^{-2}$ for set 1 and $0.0055\ \text{nm}^{-2}$ for set 2.

Tunneling into the donor layer. The applicability of our model to the Fletcher *et al.* device can be questioned because the width of the spacer layer is very small, $s = 1.67$ nm, and, therefore, tunneling of the electrons of the 2DEG into the donor layer might be non-negligible. We have performed a calculation allowing for that effect, including terms due to the electrostatic potential of the 2DEG electrons also in the donor layer up to a depth of 10 nm (counted from the spacer boundary z_2.) This makes

TABLE II. Two-dimensional electron densities for the same devices as in the previous table, but including nonvanishing acceptor densities. Cases 1 and 2, $\rho_a = 10^{-7}\ \text{nm}^{-3}$; case 3, $\rho_a = 3.10^{-7}\ \text{nm}^{-3}$. The different approximations are discussed in the text.

	Case 1		Case 2		Case 3	Set 1
	$\tilde{\sigma}_-$	σ_-	$\tilde{\sigma}_-$	σ_-	$\tilde{\sigma}_-$	σ_-
Fully quantal	0.0027	0.0022	0.0046	0.0042	0.0060	0.0053
Thomas-Fermi	0.0026	0.0024	0.0051	0.0047	0.0068	0.0061
TF + linear	0.0027	0.0023	0.0052	0.0047	0.0063	0.0056

equations such as (19) inappropriate, and the numerical process becomes considerably more involved. Our results for such a calculation can be summarized as follows: (a) σ_- is unchanged. (b) We find two bound solutions to Eq. (8), whose energies differ by less than 1 meV from those obtained when no tunneling into the donor layer is allowed. The wave functions for the lowest solution with and without tunneling are indistinguishable in the spacer and the substrate, and the tunneling into the donor layer is strongly damped. The changes are noticeable for the second bound wave function, the main effect of allowing for tunneling being an overall shift by 2 to 3 nm of the shape of the wave function towards the donor layer. However, since that state is very weakly bound the corresponding occupation factor, ν, is always small and these changes have little effect on the total electron distribution. We therefore omit any further discussion of this more involved calculation.

The structure of the donors. In developing the previous three cases we have not set out explicitly the assumed nature of the donor centers. We have tried only to give a broad coverage of the different cases that have been already considered in the literature. But although the subject is still somewhat controversial, there appears to be a growing consensus on the nature of the deep donors or DX centers and a better understanding of their properties.[8] Therefore, we wish to emphasize that *the above methods are quite appropriate to describe donor layers containing such centers in full or in part, if the validity of the model proposed by Chadi and Chang is confirmed.* The mechanism invoked by these authors for the formation of a DX center is $2d^0 \to d^+ + DX^-$, so that in a Si doped $Al_xGa_{1-x}As$ alloy with $x > 0.22$ it is energetically favorable to form, out of a pair of neighboring neutral Si atoms (d^0), one positively ionized Si (d^+) and one negatively ionized DX^- center. When the latter is ionized $DX^- \to d^+ + 2e^-$, one is left with two electrons and two positively ionized d^+ centers. The distribution of charge after ionization is thus identical to that which would be found for, e.g., shallow donors, provided there is enough energy available for the ionization of the DX center: two Si^+ ions remain in the donor layer and two electrons are transferred to the 2DEG. Let us now consider specifically the model heterostructure used to illustrate the case 1 devices: The conduction band edge is shown in Fig. 1(a). It can be seen that it has a minimum in the donor layer of about 165 meV. If, to specify a model parameter not given by Tan *et al.*, we make the assumption that in this heterostructure the DX center ionization energy is smaller than that, say 150 meV, then the full ionization condition is indeed appropriate and the case 1 model is perfectly suitable for this device. For other parameters it may happen that the full ionization conditions do not apply. This is why we have considered in detail case 3 for the devices of Fletcher *et al.* The assumed ionization energy of the deep donor level considered in this Case is of $\simeq$ 180 to 190 meV, which are typical values found for a DX center, so that this model is appropriate for a donor layer where only part of the DX centers have emitted their electrons.

Of course in that part of the donor layer where the energy is not sufficient for ionization, pairs of d^+ and DX^- centers will remain. However, the mechanism of formation guarantees that the members of each pair are close enough that one can safely neglect their mutual distance in computing the electrostatic potential, and assume zero net charge. Note that this is very similar to the approximation made when the charges of each individual ion in the ionized donor layer are replaced by a uniform distribution.

III. THOMAS-FERMI APPROXIMATION FOR THE ELECTRON GAS

We turn to this approximation guided by its success in atomic physics, mainly in the prediction of global properties of the atom and their dependence on parameters governing the bulk behavior of the system, such as variation in the size of the atom with respect to number of electrons, etc. Here we try to obtain estimates for a bulk quantity like σ_-, rather than an accurate description of the electron distribution along the z axis (whose analogue in the atomic case would be the radial electron distribution). We find good results not only for the 2D density but also for the z dependent electrostatic potential seen by the electrons, so that the Thomas-Fermi solution turns out to be also a useful starting point for the iterative solution of the fully quantal problem.

We begin by making the conventional approximation for a 3D electron Fermi gas at zero temperature, so that the local potential and density are related by

$$\rho_e(z) = \frac{1}{3\pi^2}\left(-\frac{2m^*}{\hbar^2}\, e\Phi(z)\right)^{3/2} \Theta[-e\Phi(z)]. \qquad (22)$$

From the results in the previous section we expect the Thomas-Fermi density to be nonvanishing only in the substrate. We thus focus on this layer, and omit the Heaviside function from now on. In addition, in the following the quantities computed at $z = z_3$ will be understood to correspond to the values in the substrate and not in the spacer as in the preceding section. The Poisson equation, therefore, reads

$$e\Phi''(z) = -\frac{e^2}{3\pi^2\varepsilon}\left(\frac{2m^*}{\hbar^2}\right)^{3/2} [-e\Phi(z)]^{3/2}, \qquad (23)$$

where we neglect the small difference between the dielectric constants ε_1 and ε_2, and set $\varepsilon = \varepsilon_1$ everywhere. The above relation is an ordinary second order differential equation whose solution is analytic. We obtain it in two steps to introduce more easily the appropriate boundary conditions. Set

$$\alpha = \frac{e^2}{3\pi^2\varepsilon}\left(\frac{2m^*}{\hbar^2}\right)^{3/2}, \qquad v(z) = -e\Phi(z)\,. \qquad (24)$$

One finds immediately that

$$v'(z)^2 = v'(z_3)^2 + \tfrac{4}{5}\alpha[v(z)^{5/2} - v(z_3)^{5/2}]\,. \qquad (25)$$

Since we are interested only in those solutions which cor-

respond to vanishing charge when $z \to \infty$, this requires that $e\Phi'(z)$ should also vanish in that limit, and imposes a boundary condition that is fulfilled if

$$v'(z_3) = -\sqrt{\frac{4\alpha}{5}}v(z_3)^{5/4}. \quad (26)$$

This involves quantities that we have shown in the previous section to depend on only one independent unknown, so that this equation allows one to determine these quantities. Choosing σ_- as the unknown, Eq. (26) reads

$$\frac{e^2}{\varepsilon}\sigma_- = \sqrt{\frac{4\alpha}{5}}\left\{-e\phi_s + \frac{e^2}{\varepsilon}\left[\frac{1}{2}\rho_c c^2 + \rho_d\left(c+\frac{d}{2}\right)d - \sigma_- z_3\right]\right\}^{5/4}, \quad (27)$$

in case 1, whereas, for case 2 one finds instead

$$\frac{e^2}{\varepsilon}\sigma_- = \sqrt{\frac{4\alpha}{5}}\left[e\Phi_b - e\Phi_i - \frac{e^2}{\varepsilon}\left(\frac{\sigma_-^2}{2\rho_d} + \sigma_- s\right)\right]^{5/4}. \quad (28)$$

Both equations are easily solved numerically using the Newton-Raphson method. This is the only numerical step in this TF approximation, replacing the cumbersome self-consistent process of the preceding section. This simplicity is maintained in case 3, but the explicit expressions are a bit more involved. We found it convenient to choose u as the unknown, and then placing in Eq. (26) the results of Eqs. (20), (19) and (16), one finds an analytic expression of similar structure to that of the two equations above that can again be solved using the Newton-Raphson method.

The Thomas-Fermi predictions for the three devices studied in the preceding section are shown in Table I. It can be seen that in all cases there is a satisfactory agreement with the fully quantal result. However, what is particularly interesting is the ability of the TF approximation to reproduce the changes in σ_- when the physical properties of a given device are modified: we have performed a series of calculations in each of which one of the parameters of the Tan *et al.* device is varied by a sizeable amount and find that in all cases the TF predictions are remarkably accurate. Some examples (Thomas-Fermi values given in parentheses) are (1) changing the width of the donor layer to $d = 25$ nm leads to $\sigma_- = 0.0060(0.0060)$ nm^{-2}, (2) changing the width of the spacer layer to $s = 10$ nm leads to $\sigma_- = 0.0024(0.0023)$ nm^{-2}, (3) choosing $\rho_c = \rho_d = 0.001\,25$ nm^{-3} gives $\sigma_- = 0.0059(0.0059)$ nm^{-2}, (4) changing the width of the cap layer to $c = 20$ nm leads to $\sigma_- = 0.0059(0.0060)$ nm^{-2}.

Another example of the capability of the TF model to describe systematic trends is shown in Fig. 2, where the reference device chosen is that of set 2 of Fletcher *et al.* and σ_- is plotted against different values of the spacer thickness, s. The agreement for the larger values of s is particularly good, and deteriorates somewhat when $s \leq 3$ nm, but even for these values the change of slope is

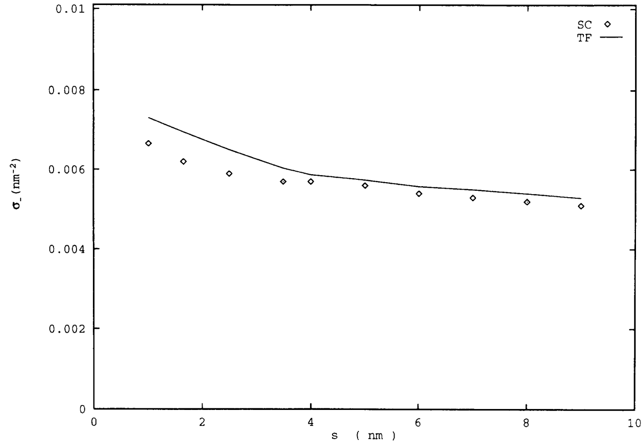

FIG. 2. Two-dimensional electron density vs spacer thickness. The other device parameters are those of set 2 of Fletcher *et al.*

correctly given and in both calculations the same trend is found.

The potential in the Thomas-Fermi approximation. Integrating Eq. (25), the explicit analytic form of the potential in the substrate is found to be

$$e\Phi(z) = -\left([-e\Phi(z_3)]^{-1/4} + \sqrt{\frac{\alpha}{20}}(z_3 - z)\right)^{-4}, \quad (29)$$

whose parameters are completely determined by the solutions to the previous equations. For the other layers the same analytic expressions as for the fully quantal case apply. The results for the devices taken as reference are shown in Figs. 1(a) to 1(c) (dashed lines.) Comparison with the fully quantal curves shows that although the shapes are always very close, the Thomas-Fermi potential in the substrate is systematically shifted upwards.

Approximate analytic solutions for σ_-. In case 1, and for the usual values of the parameters, it is easy to check that the right-hand side (rhs) of Eq. (27) varies almost linearly with σ_- in the interval $0 < \sigma_- < \sigma_0$, the latter being the value for which that term vanishes:

$$e\phi_s - \frac{e^2}{\varepsilon}\left[\frac{1}{2}\rho_c c^2 + \rho_d\left(c+\frac{d}{2}\right)d - \sigma_0 z_3\right] = 0. \quad (30)$$

Therefore, the rhs of Eq. (27) can be well approximated by a straight line passing through these two points:

$$\left\{-e\phi_s + \frac{e^2}{\varepsilon}\left[\frac{1}{2}\rho_c c^2 + \rho_d\left(c+\frac{d}{2}\right)d - \sigma_- z_3\right]\right\}^{5/4} \simeq \left\{-e\phi_s + \frac{e^2}{\varepsilon}\left[\frac{1}{2}\rho_c c^2 + \rho_d\left(c+\frac{d}{2}\right)d\right]\right\}^{5/4} \times\left(1 - \frac{\sigma_-}{\sigma_0}\right). \quad (31)$$

Placing this linear approximation in Eq. (27) one solves for σ_- and finds

$$\sigma_{-,\mathrm{la}} = \frac{\sigma_0}{1+\frac{1}{\Lambda}}, \quad (32)$$

where

$$\Lambda \equiv \sqrt{\frac{4\alpha}{5}} \left\{ -e\phi_s + \frac{e^2}{\varepsilon} \left[\frac{1}{2}\rho_c c^2 + \rho_d d\Big(c + \frac{d}{2}\Big) \right] \right\}^{1/4} z_3. \tag{33}$$

These two equations provide the desired analytic approximation to σ_- and as we will see below their predictions are remarkably accurate. However, we want first to discuss their physical interpretation. The meaning of σ_0 is simple: the left hand side of Eq. (30) is the potential drop from the surface to the junction including the contribution of an electron gas of zero width and density σ_0 located at the junction ($z = z_3$), and which satisfies the charge neutrality condition, Eq. (6). Therefore, Eq. (30) is the condition that a strictly two-dimensional electron distribution would have to satisfy to guarantee the vanishing of the total potential at infinity (and everywhere in the substrate in this particular case). Note next that since Λ in Eq. (33) is positive, the denominator in Eq. (32) is greater than one, and thus $\sigma_{-,\text{l.a.}} < \sigma_0$ always. In other words since the real electron gas has a finite thickness, the total charge required to bring $e\Phi(z)$ to zero when $z \to \infty$ is always smaller than that for a zero width gas. The reason for this reduction can be easily visualized in the following rather simplified model of the electron gas: assume that all the electrons are located in a slab between z_3 and z_3+w, with constant density, $\rho_- = \sigma_w/w$, and with σ_w satisfying the charge neutrality condition. In this model, the requirement: $e\Phi(z > z_3+w) = 0$ leads to

$$\sigma_w = \frac{\sigma_0}{1 + \frac{w}{2z_3}}, \tag{34}$$

which is of the same form as the linear approximation result and confirms the physical interpretation of the inequality $\sigma_- < \sigma_0$. Still this same model gives some physical support to the definition of an effective thickness, w_{eff}, for the true electron gas by equating the rhs of Eqs. (32) and (34), leading to

$$w_{\text{eff}} = 2z_3/\Lambda, \tag{35}$$

and, in particular, to the "reasonable" value, $w_{\text{eff}} = 10.6$ nm, for the device of Tan *et al.*

The physical parameters characterizing a device, like donor densities and thicknesses of the layers appear explicitly in expressions (32) and (33), so that their role in determining σ_- is clear. Note, for instance, that the band offset, $e\Phi_b$, does not appear explicitly, as was the case already in Eqs. (27) and (28), so that the Thomas-Fermi results are only sensitive to the value of $e\Phi_b$ to the extent that it determines whether the device has to be described as case 1 or case 2. More will be said on the role of the other parameters in the case 2 configuration, which we will discuss later. The numerical estimate given by Eqs. (32) and (33) for the Tan *et al.* device is shown in Table I: it happens to coincide with the exact quantal result. More representative of the average accuracy of these expressions are the predictions for the modified devices already considered when studying the accuracy of TF. The values predicted by the linear approximation turn out to be (1) 0.0063 nm^{-2}, (2) 0.0025 nm^{-2}, (3) 0.0062 nm^{-2}, and (4) 0.0063 nm^{-2}. The differences with TF are, thus, typically less than 5%.

In the partial ionization case the linear approximation is also found to be useful. We approximate the rhs of Eq. (28) as

$$\left[e\Phi_b - e\Phi_i - \frac{e^2}{\varepsilon}\left(\frac{\sigma_-^2}{2\rho_d} + \sigma_- s\right)\right]^{5/4} \simeq (e\Phi_b - e\Phi_i)^{5/4}\left(1 - \frac{\sigma_-}{\sigma_0}\right), \tag{36}$$

where, now, σ_0 is defined by the condition

$$e\Phi_b - e\Phi_i - \frac{e^2}{\varepsilon}\left(\frac{\sigma_0^2}{2\rho_d} + \sigma_0 s\right) = 0. \tag{37}$$

Solving Eq. (28) with this approximation we find

$$\sigma_{-,\text{l.a.}} = \left[\frac{1}{\frac{\varepsilon}{e^2}\sqrt{\frac{4\alpha}{5}}(e\Phi_b - e\Phi_i)^{5/4}} + \frac{1}{-\rho_d s + \rho_d\sqrt{s^2 + \frac{2\varepsilon(e\Phi_b - e\Phi_i)}{e^2\rho_d}}} \right]^{-1}. \tag{38}$$

Here, too, the simplicity of the explicit expression makes it easy to study the role of each parameter analytically. For instance, one finds that $\sigma_{-,\text{l.a.}}$ increases when one of the following changes happens: (a) $e\Phi_b - e\Phi_i$ increases, (b) the thickness of the spacer layer, s, decreases, (c) the donor density, ρ_d, increases (in this case, however, the thickness $t \equiv z_2 - z_r$ of the ionized layer decreases). The prediction of this approximation for the device of Laux *et al.* is also shown in Table I: again, it can be seen that the agreement with the TF result is excellent.

The same linear approximation for $[-e\Phi(z_3)]^{5/4}$ can be implemented for case 3 devices. However the expressions for σ_0 and for the value of $e\Phi(z_3)$ when σ_- is set to zero are no longer analytic. Combining Eqs. (15), (18), and (20) one can find an analytic but cumbersome expression for $u = u(\sigma_-)$. Then $v(z_3)$ can be computed for a given σ_-, but there is no analytic solution for σ_0, which has to be determined numerically. Still an expression formally identical to Eq. (32) applies again and once σ_0 is known it determines the corresponding $\sigma_{-,\text{l.a.}}$. Values for the two parameter sets of the Fletcher *et al.* device are given in Table I, showing that the accuracy of the linear approximation is satisfactory in this case as well.

IV. HETEROSTRUCTURE WITH A GATE COVERING ITS SURFACE COMPLETELY

This configuration can be studied by introducing a small formal change in the previous expressions: a gate at a negative potential, V_g, relative to the substrate pushes the conduction band at the surface upwards by eV_g. Therefore the form of Eq. (1) appropriate for this new boundary condition is just

$$e\Phi(0 < z \le z_1) = eV_g + e\phi_s - e^2\frac{\sigma_s}{\varepsilon_1}z + e^2\frac{\rho_c}{2\varepsilon_1}z^2, \tag{39}$$

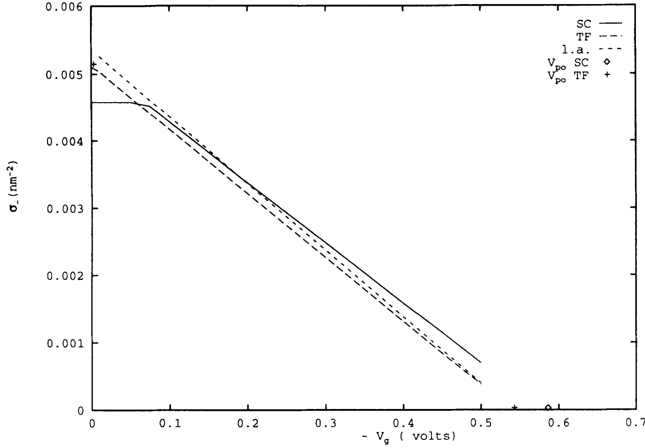

FIG. 3. Variation of the two-dimensional electron density with gate potential (absolute values) for the Laux *et al.* (Ref. 6) device. Continuous line, fully quantal result; dashed line, Thomas-Fermi prediction; double dashed line, linear approximation to TF. The diamond and the cross on the x axis mark the position of the pinch-off potentials.

and all the subsequent expressions remain the same except for the replacement of $e\phi_s$ wherever it appears by $eV_g + e\phi_s$. As an application of our methods we show in Fig. 3 the variation of σ_- vs V_g, for the fully quantal and the Thomas-Fermi approximations. Again, the predictive power of these approximations is quite apparent. The transition from case 2 to case 1 behavior can be easily seen in the line corresponding to the quantal calculation. The Thomas-Fermi results do show also this transition, but it takes place when V_g is much closer to zero. In the linear approximation the change produces a discontinuity: the case 1 behavior is indicated by the cross at $V_g \simeq 0$.

Note that, as already shown by Davies,[7] the pinch-off potential can be obtained directly from Eqs. (1) and (2) by requiring $V_{g,\text{po}}$ to be such that $e\Phi(z \geq z_3) = 0$. Since then the electron density, $\rho_e(z)$, and the electric fields in the spacer and in the substrate all vanish, from the above equations one easily obtains that

$$eV_{g,\text{po}} = -e\phi_s + e^2\left(\frac{\rho_c}{\varepsilon_1}\frac{c^2}{2} + \frac{\rho_d}{\varepsilon_1}cd + \frac{\rho_d}{\varepsilon_2}\frac{d^2}{2}\right). \quad (40)$$

In Fig. 3 the value of $V_{g,\text{po}}$ is shown as a diamond, whereas the slightly different estimate shown as a cross on the x axis corresponds to the simplification made in deriving the Thomas-Fermi equations: $\varepsilon_{2,r} = \varepsilon_{1,r} = 13.2$.

V. HETEROSTRUCTURES WITH ACCEPTOR STATES IN THE SUBSTRATE

Until now we have been assuming that there were no acceptor states in the devices under study. This has allowed a simpler presentation of our method and the main results. However, under realistic conditions there is always a small but non-negligible density of acceptor states, ρ_a, in the substrate. We shall now include the effect of these states. The presence of the acceptors fixes the asymptotic value of the electrostatic potential in the substrate, when $z \geq z_a$:

$$e\Phi(z \geq z_a) = E_g - E_a, \quad (41)$$

where E_g and E_a are, respectively, the forbidden band gap and the acceptor's binding energy (referred to the top of the valence band), and z_a is the limit of the depletion layer, that is, the lowest z that satisfies Eq. (41). The effect of the donor states is to capture electrons that otherwise would have been in the electron gas or in the donor layers, so that the contribution of an additional negatively charged layer, $[z_3, z_a]$, with constant density ρ_a has to be included in the expressions derived in previous sections. It can be checked that formally Eqs. (1)–(3) remain unchanged, whereas Eq. (4) for the potential in the substrate now contains an additional contribution:

$$e\,\delta\Phi(z_3 < z \leq z_a) = -e^2\frac{\rho_a}{2\varepsilon_1}(z - z_3)^2. \quad (42)$$

Due to the smallness of the usual acceptor densities, typically $\rho_a \simeq 10^{-7}$ nm^{-3}, the density of the electron gas is much bigger than ρ_a for z close to z_3, but since it decreases exponentially when $z \to \infty$, at large z the situation is reversed and ρ_e becomes completely negligible compared to ρ_a. Therefore, it is useful for the numerical computation to introduce a point z_4 beyond which ρ_e can be taken as vanishing for all practical purposes. (At this point the numerical integration of the Schrödinger equation is stopped.) Beyond z_4

$$e\Phi(z_4 \leq z \leq z_a) = e\Phi(z_4) + e\Phi'(z_4)(z - z_4) - e^2\frac{\rho_a}{2\varepsilon_1}(z - z_4)^2, \quad (43)$$

and applying Gauss's theorem to the slab $[z_4, z_a]$

$$e\Phi'(z_4) = e^2\frac{\rho_a}{\varepsilon_1}(z_a - z_4). \quad (44)$$

Particularizing Eq. (43) to $z = z_a$, one finds

$$z_a = z_4 + \sqrt{\frac{2\varepsilon_1[E_g - E_a - e\Phi(z_4)]}{e^2\rho_a}}, \quad (45)$$

which determines z_a in terms of z_4. Then

$$\sigma_a = \rho_a(z_a - z_3) \quad (46)$$

and the total negative charge in the substrate is

$$\tilde{\sigma}_- = \sigma_- + \sigma_a. \quad (47)$$

This new charge density, $\tilde{\sigma}_-$, now replaces σ_- in the charge neutrality conditions previously written, Eqs. (6), (12), and (21). With these additional terms one can repeat the same self-consistent processes described in the previous sections for the three cases considered, without further modification. As an illustration of the results found, the conduction band edges for the same three devices previously considered are shown in Fig. 4, with acceptor densities corresponding to those quoted by Laux *et al.* and Fletcher *et al.* for cases 2 and 3, respectively, and with $\rho_a = 10^{-7}$ nm^{-3} for case 1. The profiles are very similar to those found for vanishing acceptor densi-

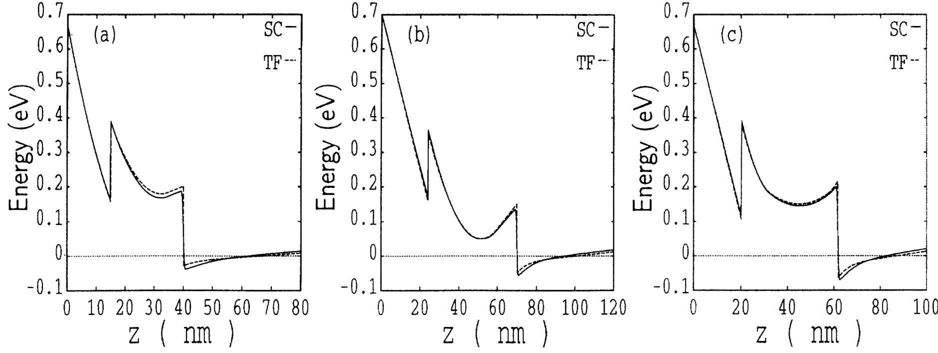

FIG. 4. Same as Fig. 1, but including effect of acceptor states.

ties except in the substrate: away from the junction the linear increase due to the electric field of the negatively charged acceptors is clearly seen. Numerical results for the two-dimensional charge densities are given in Table II. In all cases studied, the values for $\tilde{\sigma}_-$, are very close to those found for σ_- in absence of acceptor states, so that the main effect of these states is to transfer part of the negative charge from the gas to the acceptor traps.

The results for the two-dimensional density for cases 2 and 3 are in good agreement with those quoted in the original references. It should be stressed however, that for the case 3 device we determine these electron densities self-consistently without resorting to further approximations. This appears to be in contradiction to the method apparently followed by Fletcher *et al.*[3] since, as indicated in the caption of their Fig. 8, they replace the potential in the substrate by a linear approximation that does not appear to satisfy the correct asymptotic behavior at $z \to \infty$. In addition, reading from what is shown in the same figure, it appears that Fletcher *et al.* use a different value for the binding energy of the surface states, $e\phi_s$. Therefore, it is likely that the agreement between the two calculations is in part fortuituous.

The Thomas-Fermi model. The use of this approximation now requires a careful discussion of some additional approximations. The Poisson equation in the substrate reads

$$\frac{d^2 e\Phi}{dz^2} = -\frac{e^2}{\varepsilon}[\rho_e(z) + \rho_a], \tag{48}$$

and, again, it is convenient to consider two separate zones. We will assume that a z_t exists such that for $z < z_t$, the acceptor density ρ_a on the r.h.s. of the Poisson equation can be neglected compared to the Thomas-Fermi $\rho_e(z)$. Under these conditions the same derivation made in the no-acceptor case can be formally repeated and one recovers Eq. (25). However the boundary conditions at $z = z_3$ and $z = z_t$ must now be redefined. Since one wants to determine the full electrostatic potential, the electric field and potential at $z = z_3$ must be constructed so as to include the contribution of the negatively charged acceptor states. This is guaranteed when the charge neutrality condition, including their contribution, is imposed. Thus, e.g., we now require $-v'(z_3) = e\Phi'(z_3) = (e^2/\varepsilon)\,\tilde{\sigma}_-$.

To discuss the boundary conditions at $z = z_t$, we particularize Eq. (25) to this point:

$$v'(z_3)^2 - v'(z_t)^2 = \frac{4}{5}\alpha[v(z_t)^{5/2} - v(z_3)^{5/2}]. \tag{49}$$

Let us make more precise now the choice of z_t, fixing it by the condition that the solution of the above differential equation be such that

$$v'(z_t) = -e\Phi'(z_t) = -\frac{e^2}{\varepsilon}\sigma_a. \tag{50}$$

In doing so we have again neglected the small amount of acceptor charge in the interval $[z_3, z_t]$. With this choice of z_t, the left-hand side of Eq. (49) is proportional to the difference between the squares of the densities $\tilde{\sigma}_-$ and σ_a. For the small values of ρ_a that we are considering it is, therefore, quite safe to neglect the second term, $v'(z_t)^2$, compared to the first, $v'(z_3)^2$. A similar argument can be applied to the rhs of Eq. (49), so that after making these approximations the boundary condition that results is again formally the same as Eq. (26) but now both members include the contribution of $\tilde{\sigma}_-$ instead of σ_-. The derivation of the equations appropriate for the different cases now proceeds as in the no-acceptors case, and the new Eqs. (27) and (28) are also formally identical to the old ones, but again with the replacement of σ_- by $\tilde{\sigma}_-$. Correspondingly, the numerical values now determined for $\tilde{\sigma}_-$ are identical to those for σ_- in the no-acceptor case. Being consistent with the previous approximations we determine the two-dimensional acceptor density as

$$\sigma_a = \sqrt{\frac{2\varepsilon\rho_a(E_g - E_a)}{e^2}}, \tag{51}$$

and this gives for the two-dimensional density of the electron gas

$$\sigma_- = \tilde{\sigma}_- - \sigma_a. \tag{52}$$

The numerical predictions are included in Table II, and the conduction band edge profiles are also shown in Fig. 4.

VI. SUMMARY AND CONCLUSIONS

The present work has focused on the description of the electron charge distribution and conduction band edge profiles in GaAs/$Al_xGa_{1-x}As$ heterostructures. First, we have presented the fully quantal description of de-

vices with different degrees of ionization of the donor layer, and have formulated an efficient method for their self-consistent solution. Next, we have developed simpler but still sufficiently accurate models for the study of the systematics of the two-dimensional electron density. We have shown that the Thomas-Fermi approximation is well suited for these purposes, and that when complemented with a linear approximation it provides analytic expressions that relate the 2DEG density to the physical parameters of the heterostructure. These expressions make very transparent the effect of changes in the characteristics of the layers on the properties of the 2DEG.

ACKNOWLEDGMENTS

We are grateful to NSERC Canada for continued support under research Grant No. OGP00-3198 (DWLS). The work of J.M. was supported under Grant No. PB91-0236 of DGICYT, Spain.

---

[1]F. Stern and S. Das Sarma, Phys. Rev. B **30**, 840 (1984).

[2]I.-H. Tan, G.L. Snider, L.D. Chang, and E.L. Hu, J. Appl. Phys. **68**, 4071 (1990).

[3]R. Fletcher, E. Zaremba, M. D'Iorio, C.T. Foxon and J.J. Harris, Phys. Rev. B **41**, 10 649 (1990).

[4]P.M. Mooney, N.S. Caswell, and S.L. Wright, J. Appl. Phys. **62**, 4786 (1987).

[5]L. Hedin and B.I. Lundqvist, J. Phys. C **4**, 2064 (1971).

[6]S.E. Laux, J.D. Frank, and F. Stern, Surf. Sci. **196**, 101 (1988).

[7]John H. Davies, Semicond. Sci. Technol. **3**, 995 (1988).

[8]D.J. Chadi, Phys. Rev. B **46**, 6777 (1992); S.B. Zhang and D.J. Chadi, Phys. Rev. B **42**, 7174 (1990); D.J. Chadi and K.J. Chang, *ibid.* **39**, 10 063 (1989); P.M. Mooney, J. Appl. Phys. **67**, R1 (1990).